Automatic computation

of helicity amplitudes

and cross sections

Costas G. Papadopoulos

ACAT 2000

- **Need**

  Reliable cross section computation and event generation for multiparticle (≤ 10) porcesses.

- **Result**

  - **HELAC:** A.Kanaki and C.G.Papadopoulos, hep-ph/0002082.

    Matrix element computation algorithm, based on Dyson-Schwinger equations, including: EWK, QCD, fermion masses, reliable arithmetic, running couplings and masses ....

  - **PHEGAS:** C.G.Papadopoulos, LEP2Y2K, hep-ph/0007335

    Monte-Carlo phase space integration/generation based on optimized multichannel approach.

- Give the process

$$e^- e^+ \to \mu\, \bar{\nu}_\mu\, u\, \bar{d}\, \gamma\, \gamma$$

- Define the cuts

$$E_i > E_0 \quad \cos\theta_i < c_0 \quad \cos\theta_{ij} < c_1$$

- The cross section is:

$$\sigma = 1.73(5)\ \text{fb} \ \ \text{at}\ \sqrt{s} = 500\ \text{GeV}$$

- **... plus any other kinematical distribution !**

Old Feynman graphs $\to$ computational cost $\sim n!$

New Dyson-Schwinger $\to$ computational cost $\sim 3^n$

P.Draggiotis, R.H.Kleiss and C.G.Papadopoulos, Phys. Lett. B439 (1998) 157

F. Caravaglios and M. Moretti, Phys. Lett. B358 (1995) 332

- *Example:* $e^-e^+ \to e^-e^+e^-e^+$ in QED:

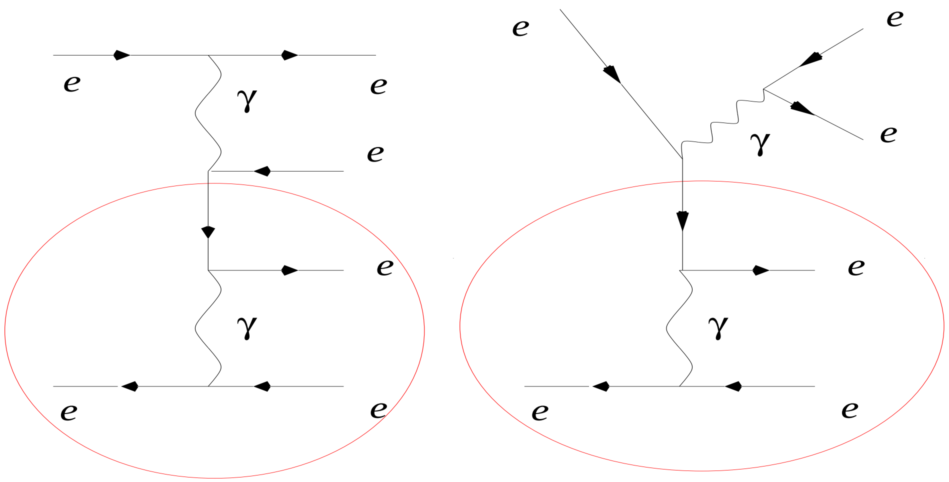

$\Rightarrow$ Systematic approach:

$b_\mu(P) =$ 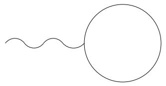 $\psi(P) =$ 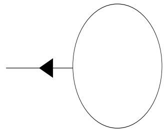 $\bar{\psi}(P) =$ 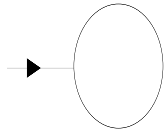

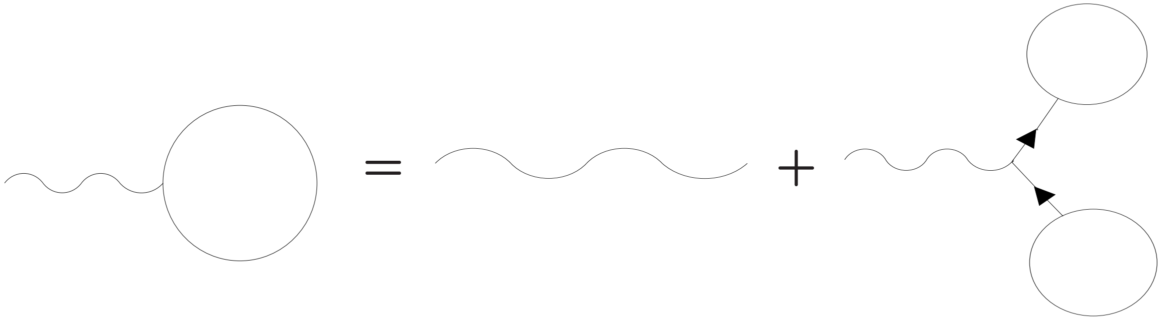

$$b^\mu(P) = \sum_{i=1}^{n} \delta_{P=p_i} b^\mu(p_i) + \sum_{P=P_1+P_2} (ig)\Pi^\mu_\nu \; \bar{\psi}(P_2)\gamma^\nu \psi(P_1)\epsilon(P_1, P_2)$$

- Let n external particles with momenta $p_i^\mu, i = 1\ldots,n$, and define the momentum P^μ

$$P^\mu = \sum_{i\in I} p_i^\mu \ , \qquad I \subset \{1,\ldots,n\}$$

- the binary vector $\vec{m} = (m_1,\ldots,m_n)$, where its components take the values 0 or 1 :

$$P^\mu = \sum_{i=1}^{n} m_i \, p_i^\mu \ .$$

- Moreover this binary vector can be uniquely represented by the integer

$$m = \sum_{i=1}^{n} 2^{i-1} m_i \ , \quad 0 \leq m \leq 2^n - 1$$

- Replace

$$b_\mu(P) \rightarrow b_\mu(m) \ .$$

- **Convenient ordering of integers in binary representation $\Rightarrow$ level l, defined by**

$$l = \sum_{i=1}^{n} m_i \; .$$

- **external momenta are of level 1**
- **the total amplitude corresponds to the unique level n integer $2^n - 1$**

$$\mathcal{A} = b(1) \cdot b(2^n - 2)$$

This ordering dictates the natural path of the computation : starting with level-1 sub-amplitudes, we compute the level-2 ones using the Dyson-Schwinger equations and so on up to level $n - 1$

The solution

$$e^-(1)\ \ e^+(2) \to e^-(4)\ \ \bar{\nu}_e(8)\ \ u(16)\ \ \bar{d}(32)$$

1	10	33	2	-2	8	1
1	12	33	4	-2	8	1
1	48	34	16	-3	32	4
2	26	-4	10	33	16	-3
			...			
2	62	-2	10	33	52	-1
2	62	-2	12	33	50	-1
2	62	-2	58	31	4	-2
2	62	-2	58	32	4	-2
2	62	-2	60	31	2	-2
2	62	-2	60	32	2	-2

- Dirac algebra simplification: 2-dim vs 4-dim and chiral representation, including $m_f \neq 0$.
- The sign factor:

$$\epsilon(P_1, P_2) \to \epsilon(m_1, m_2)$$

  we define

$$\epsilon(m_1, m_2) = (-1)^{\chi(m_1, m_2)}$$

$$\chi(m_1, m_2) = \sum_{i=n}^{2} \hat{m}_{1i} \left(\sum_{j=1}^{i-1} \hat{m}_{2j} \right)$$

  where hatted components are set to 0 if the corresponding external particle is a boson.

- Full EWK theory, both Unitary and Feynman gauges.

A. Denner, Fortsch. Phys. 41, 307 (1993).

Colour Configuration - EWK⊕QCD

- ⋆ quarks $1 \ldots n$
- ⋆ antiquarks $\sigma_i(1 \ldots n)$ and
- ⋆ gluons $= q\bar{q}$

Each color-configuration amplitude is proportional to

$$D_i = \delta_{1,\sigma_i(1)}\delta_{2,\sigma_i(2)} \cdots \delta_{n,\sigma_i(n)}$$

where σ_i represents the i-th permutation of the set $1, 2, \ldots, n$.

$$\mathcal{C}_{ij} = \sum D_i D_j = N_c^{\alpha} \ , \quad \alpha = \langle \sigma_1, \sigma_2 \rangle$$

♠ exact color treatment ⇒ low color charge

HELAC - the code

- A two-phase computation
  - phase A: selection and tree-construction (integer arithmetic)
  - phase B: computation (high-precision arithmetic)
- Comparisons: full technical agreement
  - EXCALIBUR $m_f = 0$ comparable speed
  - MADGRAPH $m_f \neq 0$ comparable speed for $n < 7$.
- As expected HELAC shows an exponential (instead of factorial) CPU-time growth. F.A.Berends, C.G.Papadopoulos and R.Pittau, hep-ph/0002249.
- There is no a priori limitation for the number of particles that HELAC can treat, the only restrictions being that of memory allocation.

Numerical reliability

- Problem due to huge 'gauge' cancellations !
- In order to have a taste of a multi-precision computation we have computed the squared amplitude for the process

$$e^-(p_1)e^+(p_2) \to e^-(p_3)e^+(p_4)e^-(p_5)e^+(p_6)$$

at two phase space points.

- Phase space point (A) is just a randomly generated one by the phase-space generator `RAMBO`.
- Phase space point (B)

$$\begin{aligned} &p_1^0/\text{ GeV} = 100,\ \vec{p}_1 + \vec{p}_2 = 0, \\ &p_3^0/p_1^0 = 0.9,\ \theta_3 = 0, \\ &(p_5 + p_6)^2/(p_4 + p_5 + p_6)^2 = 0.1,\quad \theta_4 = \phi_4 = \theta_5 = \phi_5 = 0 \end{aligned}$$

with $m_e = 0.511 \times 10^{-3}$ GeV.

- **Results are provided for these points, by using the `real*8` (DP), `real*16` (QP) and 34-digit multi-precision version of the code.**

David M. Smith, Transactions on Mathematical Software 17 (1991) 273.

(A)	(B)
1.5397285231505 95E-008	1.256276706229023E+023
1.539728523150588541567630028250 13D-08	3.071626010937109151341369249730 89D+22
1.539728523150588541567630028250 11853M-8	3.071626010937109151279501092417 70808M+22

- **In the `MP`-version of the code the precision is defined by the user.**

PHEGAS

- **Phase space**

$$d\Phi_n = (2\pi)^{4-3n} \prod_{i=1}^{n} \frac{d^3 p_i}{2E_i} \delta\left(\sum E_i - w\right) \delta^3\left(\sum \vec{p}_i\right)$$

- **RAMBO, VEGAS-based nice but completely inefficient!**

$$d\sigma_n = \mathbf{FLUX} \times |\mathcal{M}_{2\to n}|^2 d\Phi_n$$

need appropriate mappings of peaking structures, plus optimization!

- **Efficiency $\Rightarrow$ to a large number of generators, each one for a specific class of processes.**

Multichannel approach

$$\mathcal{I} = \int f(\vec{x}) d\mu(\vec{x}) = \int \frac{f(\vec{x})}{p(\vec{x})} p(\vec{x}) d\mu(\vec{x})$$

$$p(\vec{x}) = \sum_{i=1}^{M_{ch}} \alpha_i \, p_i(\vec{x}) \qquad \sum_{i=1}^{M_{ch}} \alpha_i = 1$$

$$\mathcal{I} \rightarrow \left\langle \frac{f(\vec{x})}{p(\vec{x})} \right\rangle \qquad \mathcal{E}^2 N \rightarrow \left\langle \left(\frac{f(\vec{x})}{p(\vec{x})} \right)^2 - \mathcal{I}^2 \right\rangle$$

$\star$ **Optimize $\alpha_i \Rightarrow$ Minimize $\mathcal{E}$** $\star$

R.Kleiss and R.Pittau, Comput. Phys. Commun. 83, 141 (1994).

New **Dyson-Schwinger equations: subamplitude is a combination of several peaking structures!**

problem unsolved

P.D.Draggiotis, A.van Hameren and R.Kleiss, hep-ph/0004047.

Old **Feynman graphs: exhibit single peaking structure!**

problem solved

Back to Feynman graphs:

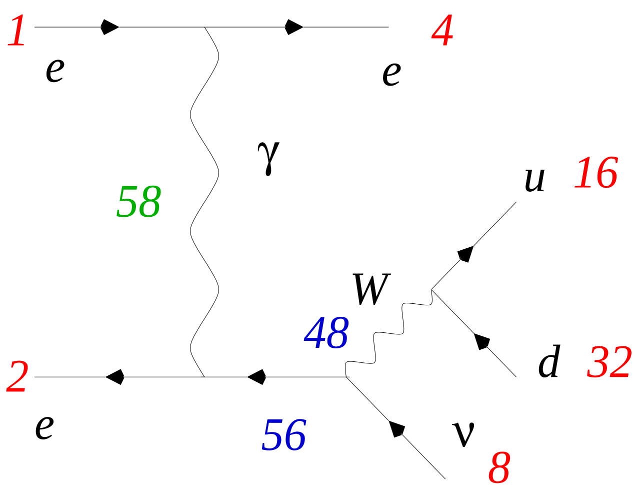

The corresponding intrinsic representation looks like

62	-2	4	-2	58	31
58	31	2	-2	56	2
56	2	48	33	8	1
48	33	16	-3	32	4

Time-like momenta $q^2 \geq 0$

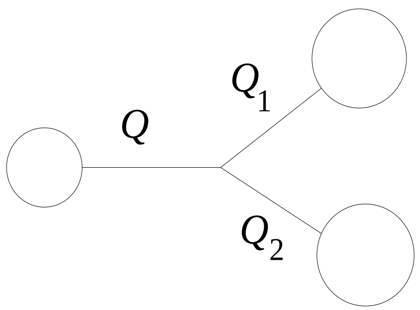

$$
\begin{aligned}
d\Phi_n &= \ldots \frac{dQ_1^2}{2\pi}\,\frac{dQ_2^2}{2\pi}\, d\Phi_2(Q \to Q_1, Q_2) \ldots \\
&= \ldots \frac{dQ_1^2}{2\pi}\,\frac{dQ_2^2}{2\pi}\, d\cos\theta\; d\phi\; \frac{\lambda^{1/2}(Q^2, Q_1^2, Q_2^2)}{32\pi^2\; Q^2} \ldots
\end{aligned}
$$

Space-like momenta

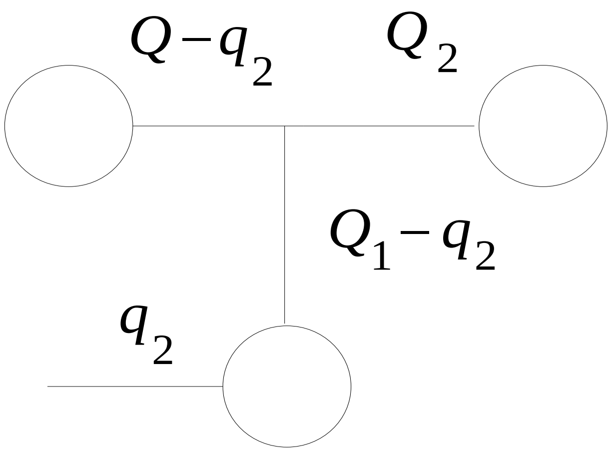

$$
\begin{aligned}
d\Phi_n &= \ldots \frac{dQ_1^2}{2\pi}\,\frac{dQ_2^2}{2\pi}\; d\Phi_2(Q\to Q_1,Q_2)\ldots \\
&= \ldots \frac{dQ_1^2}{2\pi}\,\frac{dQ_2^2}{2\pi}\; dt\; d\phi\; \frac{1}{32\pi^2\; Q\; |\vec{q}_2|}\ldots
\end{aligned}
$$

$$
t=(Q_1-q_2)^2=m_2^2+Q_1^2-\frac{E_2}{Q}(Q^2+Q_1^2-Q_2^2)+\frac{\lambda^{1/2}}{Q}|\vec{q}_2|\cos\theta
$$

- **Find limits of $t(Q_1^2, \cos\theta)$:**

$$t_\pm = m_2^2 + Q_1^2 - \frac{E_2}{Q}(Q^2 + Q_1^2 - Q_2^2) \pm \frac{\lambda^{1/2}}{Q}|\vec{q}_2|$$

In order to find the maximum of t_+ we study the function $\partial t_+/\partial Q_1^2$ in the region $Q_{1,min}^2 < Q_1^2 < (Q - Q_2)^2$. Since

$$\frac{\partial^2 t_+}{\partial (Q_1^2)^2} = -4Q^2 Q_2^2 \lambda^{-3/2} \frac{|\vec{q}_2|}{Q} \leq 0$$

and

$$\partial t_+/\partial Q_1^2|_{Q_1^2=(Q-Q_2)^2} \to -\infty$$

we just consider two cases ($|\vec{q}_2| \neq 0$):

1. $\partial t_+/\partial Q_1^2|_{Q_1^2=Q_{1,min}^2} < 0$ in which case $t_{max} = t_{+,max} = t_+(Q_1^2 = Q_{1,min}^2)$, and
2. $\partial t_+/\partial Q_1^2|_{Q_1^2=Q_{1,min}^2} > 0$ in which case one can easily derive

$$t_{max} = t_+(Q_1^2 = x_-) \text{ with}$$

$$x_- = Q^2 + Q_2^2 - 2\,Q\,Q_2 \frac{1 - E_2/Q}{\sqrt{\alpha}}\,, \quad \alpha = \left(1 - \frac{E_2}{Q}\right)^2 - \left(\frac{|\vec{q}_2|}{Q}\right)^2 > 0$$

♠ **Q_1^2-limits:**

The limits for the Q_1^2-integration for given t can now be fixed by the condition $|\cos\theta| \leq 1$ or equivalently

$$\Pi(Q_1^2) \leq 0$$

with

$$\Pi(Q_1^2) = \left(t - Q_1^2 - m_2^2 + \frac{E_2}{Q}(Q^2 + Q_1^2 - Q_2^2)\right)^2 - \left(\frac{|\vec{q}_2|}{Q}\right)^2 \lambda$$

If $y_1 \leq y_2$ are the two roots of the polynomial $\Pi(Q_1^2)$ then we have

1. For $a > 0$, $y_- < Q_1^2 < y_+$, with $y_- = \max(y_1, Q^2_{1,min})$ and $y_+ = \min(y_2, Q^2_{1,max})$
2. For $a < 0$ we have to satisfy two conditions $Q_1^2 < y_1$ or $y_2 < Q_1^2$ and $Q^2_{1,min} < Q_1^2 < Q^2_{1,max}$

- **At the end we get:**

$$d\Phi_n \to \prod ds_i \; p_i(s_i) \prod dt_j \; p_j(t_j) \prod d\phi_k \prod d\cos\theta_l$$

- $p(x)$ **are chosen so that 'singularities' are smoothed out!**

  - ♦ $(s - m^2)^2 + m^2\Gamma^2$ **for massive unstable particles,** $W^{\pm}$, Z.
  - ♦ s^{ν} **for time-like massless propagators, e.g.** γ, **gluons, fermions.**
  - ♦ $|t|^{\nu}$ **for space-like massless propagators.**

Final states	number of FG	$\sqrt{s}$ (GeV)	Cross section (fb)
$u\ \bar{d}\ s\ \bar{c}\ \gamma$	90(74)	200	199.75 (16)
$e^-\ \bar{\nu}_e\ \mu^+\ \nu_\mu\ \gamma$	108(100)	200	29.309 (25)
$\mu^-\ \bar{\nu}_\mu\ u\ \bar{d}\ \gamma\ \gamma$	587(210)	500	1.730 (58)
$\mu^-\ \bar{\nu}_\mu\ u\ \bar{d}\ c\ \bar{c}$	209(102)	500	0.1783 (20)
$\mu^-\ \bar{\nu}_\mu\ u\ \bar{d}\ c\ \bar{c}\ \gamma$	2142(339)	500	0.02451 (65)

- $g\,g \to b\,\bar{b}\,b\,\bar{b}\,W^-W^+$
  - challenging process, from a computational point of view
  - a nice example to demonstrate the ability of PHEGAS/HELAC to deal with QCD processes.
  - background of $t\bar{t}H$ production

MC points $w > 0$	result (fb)	error (fb)	efficiency (%)	efficiency $w > 0$ (%)
99442	4.716	0.024	3.3	33

  - energy $\sqrt{s} = 500$ GeV and to 1×10^6 MC points.
  - Feynman graphs for this process is 960, without taking into account electroweak contributions from Z and γ intermediate states.

Parameters used are $g_{QCD} = 1$, $m_{top} = 175$ GeV and $\Gamma_{top} = 1.5$ GeV. Moreover the following set of cuts has been applied:

$$M_{q,q'} > 20\mathrm{GeV}, \quad E_q > 20\mathrm{GeV}, \quad |\cos\theta(q, \mathrm{beam})| < 0.9,$$

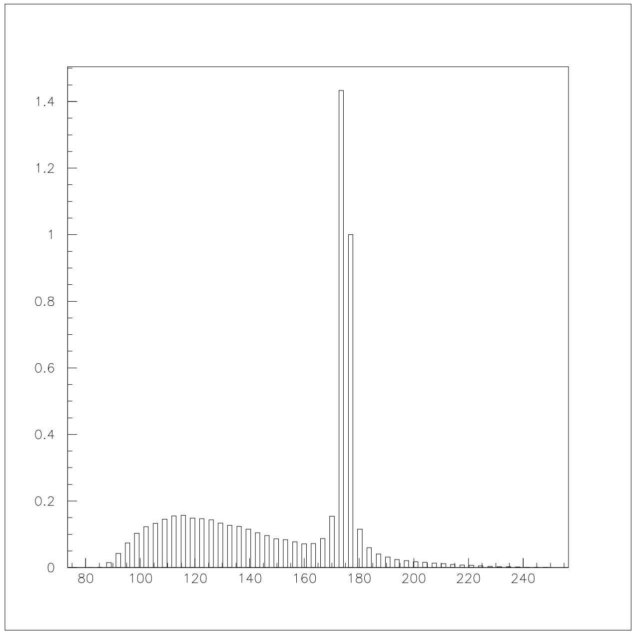

- $e^- \, e^+ \to e^- \, e^+ \, \mu^- \, \mu^+$

$\boldsymbol{\sigma_{tot}}$ **(in nb)**

$\sqrt{s}$(GeV)	BDK	NEXTCALIBUR
20	98.9 ± 0.6	99.20 ± 0.98
35	131.4 ± 2.2	131.03 ± 0.88
50	154.4 ± 0.9	152.33 ± 0.83
100	205.9 ± 1.2	204.17 ± 1.73
200	—	263.50 ± 1.31
200 (all)	—	265.58 ± 1.44

- $e^- \, e^+ \rightarrow e^- \, e^+ \, e^- \, e^+$

σ_{tot} **(in nb $\times 10^7$)**

$\sqrt{s}$(GeV)	BDK	NEXTCALIBUR
20	$0.920 \pm .011$	$0.905 \pm .011$
35	$1.070 \pm .015$	$1.079 \pm .014$
50	$1.233 \pm .018$	$1.214 \pm .016$
100	$1.459 \pm .025$	$1.485 \pm .020$
200	—	$1.776 \pm .019$
200 (all)	—	$1.787 \pm .030$

Outlook

PHEGAS/HELAC: a framework for high-energy phenomenology

- **Standard Model fully included**

⋆ **High color charge processes: multijet production**

P.Draggiotis, R.H.Kleiss and C.G.Papadopoulos, Phys. Lett. B439 (1998) 157

⇒ **New Physics effects**

- **Trilinear Gauge Couplings + Quartic**
- **SUSY and new particles**

⋆ **Higher order corrections**

- **Direct approach**
- **Running couplings and masses**

$$V^A = (V^0 + V_z, V^0 - V_z, V_x + iV_y, V_x - iV_y) \ , \quad A = 1, \ldots, 4 \ .$$

Polarization state-vectors are given by

$$\begin{aligned}
\epsilon_-^A &= \left(\frac{-p_T}{\sqrt{2}|\vec{p}|}, \frac{p_T}{\sqrt{2}|\vec{p}|}, \frac{(p_x + ip_y)(|\vec{p}| + p_z)}{\sqrt{2}|\vec{p}|p_T}, \frac{(p_x - ip_y)(-|\vec{p}| + p_z)}{\sqrt{2}|\vec{p}|p_T} \right) \\
\epsilon_+^A &= \left(\frac{p_T}{\sqrt{2}|\vec{p}|}, \frac{-p_T}{\sqrt{2}|\vec{p}|}, \frac{(p_x + ip_y)(|\vec{p}| - p_z)}{\sqrt{2}|\vec{p}|p_T}, \frac{(p_x - ip_y)(-|\vec{p}| - p_z)}{\sqrt{2}|\vec{p}|p_T} \right) \\
\epsilon_0^A &= \left(\frac{|\vec{p}|}{\sqrt{p^2}} + \frac{p_z p_0}{|\vec{p}|\sqrt{p^2}}, \frac{|\vec{p}|}{\sqrt{p^2}} - \frac{p_z p_0}{|\vec{p}|\sqrt{p^2}}, \frac{(p_x + ip_y)p_0}{|\vec{p}|\sqrt{p^2}}, \frac{(p_x - ip_y)p_0}{|\vec{p}|\sqrt{p^2}} \right)
\end{aligned}$$

As for the Dirac matrices we are using the chiral representation. The wave functions which describe massive spinors are given by:

$$u_+(p) = \begin{pmatrix} r/c \\ a(p_x + ip_y)/r \\ -mb/r \\ -m(p_x + ip_y)/r \end{pmatrix} \qquad \bar{u}_+(p) = \begin{pmatrix} mb/r \\ m(p_x - ip_y)/r \\ -r/c \\ -a(p_x - ip_y)/r \end{pmatrix}$$

$$u_-(p) = \begin{pmatrix} m(p_x - ip_y)/r \\ -mb/r \\ -a(p_x - ip_y)/r \\ r/c \end{pmatrix} \qquad \bar{u}_-(p) = \begin{pmatrix} a(p_x + ip_y)/r \\ -r/c \\ -m(p_x + ip_y)/r \\ mb/r \end{pmatrix}$$

$$v_+(p) = \begin{pmatrix} -m(p_x - ip_y)/r \\ mb/r \\ -a(p_x - ip_y)/r \\ r/c \end{pmatrix} \qquad \bar{v}_+(p) = \begin{pmatrix} a(p_x + ip_y)/r \\ -r/c \\ m(p_x + ip_y)/r \\ -mb/r \end{pmatrix}$$

$$v_-(p) = \begin{pmatrix} r/c \\ a(p_x + ip_y)/r \\ mb/r \\ m(p_x + ip_y)/r \end{pmatrix} \qquad \bar{v}_-(p) = \begin{pmatrix} -mb/r \\ -m(p_x - ip_y)/r \\ -r/c \\ -a(p_x - ip_y)/r \end{pmatrix}$$

where:

$$a = p_0 + |\vec{p}|, \quad b = p_z + |\vec{p}|, \quad c = 2|\vec{p}|, \quad r = \sqrt{abc}$$

For a massless particle the spinors are

$$u_R(p) = \begin{pmatrix} \sqrt{p_0 + p_z} \\ (p_x + ip_y)/\sqrt{p_0 + p_z} \\ 0 \\ 0 \end{pmatrix} \qquad \bar{u}_R(p) = \begin{pmatrix} 0 \\ 0 \\ -\sqrt{p_0 + p_z} \\ -(p_x - ip_y)/\sqrt{p_0 + p_z} \end{pmatrix}$$

$$u_L(p) = \begin{pmatrix} 0 \\ 0 \\ -(p_x - ip_y)/\sqrt{p_0 + p_z} \\ \sqrt{p_0 + p_z} \end{pmatrix} \qquad \bar{u}_L(p) = \begin{pmatrix} (p_x + ip_y)/\sqrt{p_0 + p_z} \\ -\sqrt{p_0 + p_z} \\ 0 \\ 0 \end{pmatrix}$$

$$V_\mu = \bar{\psi}(P_1)\gamma_\mu\left(g_R\omega_R + g_L\omega_L\right)\psi(P_2)$$

turns out to be

$$V^A = \begin{pmatrix} -g_R\psi_1\bar{\psi}_3 - g_L\psi_4\bar{\psi}_2 \\ -g_R\psi_2\bar{\psi}_4 - g_L\psi_3\bar{\psi}_1 \\ -g_R\psi_2\bar{\psi}_3 + g_L\psi_4\bar{\psi}_1 \\ -g_R\psi_1\bar{\psi}_4 + g_L\psi_3\bar{\psi}_2 \end{pmatrix}$$

where $\psi_i(\bar{\psi}_i), i = 1, \ldots, 4$ are the components of the spinor $\psi(P_2)$ $\left(\bar{\psi}(P_1)\right)$ and

$$\omega_L = \frac{1}{2}\left(1 - \gamma_5\right) \ , \quad \omega_R = \frac{1}{2}\left(1 + \gamma_5\right) \quad .$$

On the other hand, the spinor

$$u = (\not{P} + m)\not{b}(P_1)\omega_R\psi(P_2)$$

can be reduced to

$$u = \begin{pmatrix} (-b_2p_1 + b_3p_4)\psi_1 + (b_4p_1 - b_1p_4)\psi_2 \\ (b_3p_2 - b_2p_3)\psi_1 + (-b_1p_2 + b_4p_3)\psi_2 \\ m(b_2\psi_1 - b_4\psi_2) \\ m(-b_3\psi_1 + b_1\psi_2) \end{pmatrix}$$

where ψ_i, b_i, p_i, $i = 1, \ldots, 4$ are the components of P, $b(P_1)$ and $\psi(P_2)$ respectively.